Twisted-baryon-loop effects in dual topological unitarization

P. Gauron, B. Nicolescu, S. Ouvry, and J. Uschersohn*
Division de Physique Théorique,† Institut de Physique Nucléaire, Orsay, France 91406
and Laboratoire de Physique Théorique et Particules Elémentaries, Université Pierre et Marie Curie, Paris, France†
(Received 9 December 1980)

Within the framework of dual topological unitarization we propose a simple model for mesons, baryons, and baryonium which allows us to calculate the effects of inserting nonplanar $B\bar{B}$ loops in all possible ways into meson and baryonium propagators. We study the renormalization of the leading nonzero-isospin trajectories and the mixing of $q\bar{q}$ and $qq\bar{q}\bar{q}$ states.

I. INTRODUCTION

The dual-topological-unitarization (DTU) approach to hadron physics is quite successful in the case of mesons.[1] Its extension to baryons is intrinsically difficult, due essentially to the complex nature of the "topological-entropy" index, which governs the topological expansion.

Important progress in the formulation of DTU with baryons has been made in the last few years. A generalization of DTU inspired by quantum chromodynamics has shown the importance of understanding the role played in this formulation not only by baryons, but also by baryonium states.[2] Different mathematical aspects connected with the definition of a proper topological-entropy index have been studied.[3]

More recently, the necessity of considering a new "quantum" surface, viewed as the "source" of internal quantum numbers and essentially responsible for the quark confinement, has been recognized.[4] This quantum surface is two-dimensional, closed, and oriented and has to be considered in addition to the usual two-dimensional and bounded " classical" surface,[1] which describes the space-time structure of hadron collisions. A tentative definition or ordinary and multiquark hadrons, quarks, and gluons, based upon this quantum surface, has been made.[5] Finally, a complete topological-expansion theory, involving both the quantum and classical surfaces, has been formulated.[6]

The present paper addresses itself to the question of practical computations in the framework of DTU with baryons, beyond the lowest order of the topological expansion. Rigorous calculations based upon the theory formulated in Ref. 6 seem, for the moment, premature, the question of a "physical" lowest order remaining to be clarified. We choose here to approach the general problem of DTU with baryons, by formulating a simple model which includes some information coming from the quantum surface. Our model can be therefore considered as a continuation of previous efforts[2,7-10] in making practical computations in the case of DTU with baryons (but which considered only the classical surface and were devoted only to the "planar" and "cylinder" levels).

In Sec. II, we present the DTU model for baryons and baryonium that we are using. In Sec. III, we formulate a method of global calculation of "nonplanar" baryon-antibaryon loop insertions in the Reggeon propagators, some technical details of our method of calculation being given in the Appendix. A discussion of the phenomenological consequences of our calculations is given in Sec. IV.

II. A DTU MODEL FOR BARYONS AND BARYONIUM

In this paper we use the DTU model for baryons and baryonium proposed in Refs. 5 and 11. In the language of the familiar duality diagrams,[11] a quark will be represented by the solid line in Fig. 1 which is associated with two indices: i is a flavor index and σ a three-valued "topological color" index[5] ($\sigma = \{\alpha, \beta, \gamma\}$). The direction of the arrow indicates if the solid line represents a quark or an antiquark. The σ and i indices are separately associated with two other different types of lines: The wavy line in Fig. 1 represents a "topological color line" σ, while the dashed line represents a "topological flavor line" i. The rules of contraction on the quantum surface of Ref. 5 imply the connection of the three types of lines by the three-line vertices of Fig. 2. A "topological gluon" can be represented by a pair of wavy lines of opposite orientations.

Figure 3 then represents a meson (M_2), Fig. 4 a baryon (B) and Fig. 5 a baryonium (M_4). One must note that a baryon corresponds always to a clockwise order of color labels, while an antibaryon corresponds to an anticlockwise order of color labels.[5] The order of color labels is defined[11] with respect to the direction which is obtained by taking the physical direction in which the hadron as a whole is moving and rotating this clockwise through 90°. Thus Fig. 4 represents both a baryon traveling from left to right and an

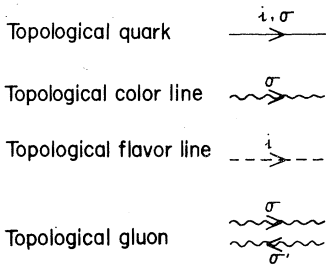

FIG. 1. Quasiplanar representation of topological quarks, color lines, flavor lines, and gluons.

antibaryon traveling from right to left. One must also note that the colors of two contiguous wavy lines are different within the baryonium state[5] (see Fig. 5).

The detailed rules for drawing the diagrams describing processes are given in Ref. 11. (Here we just note that the graphs corresponding to cyclic permutation of color labels are equivalent.)

These generalized ("quasiplanar"[11]) duality diagrams have the virtue of projecting in a compact and intuitive way the information coming both from the classical and quantum surfaces.

The main difference between the generalized duality diagrams and the usual Harari-Rosner diagrams consists in the introduction of the new topological index σ. The introduction of the topological color σ was necessary in order to obtain a consistent definition of hadrons, quarks, and gluons based upon the analysis of the quantum surface made in Ref. 5. In this sense, the model presented here can be considered as an approximate approach to the general and difficult problem of baryons in DTU.[6] This approach is, of course, rather crude and simple, but it makes possible the explicit (and hopefully realistic) calculations of nonplanar $B\bar{B}$ insertions for Reggeon propagators, as shown in the following sections.

In the lowest (planar) order of the topological expansion, none of our lines cross in diagrams describing processes. The higher-entropy components correspond to diagrams in which the quark lines cross in a well defined way, due to the *fixed* order of the color labels (clockwise in baryons and counterclockwise in antibaryons) and due to the fact that we consider here quantum surfaces without singular topological points.[12] In order to illustrate this point, we will take as an example

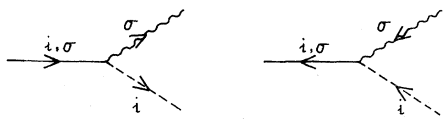

FIG. 2. Color-flavor three-line vertices.

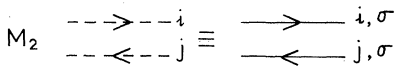

FIG. 3. Quasiplanar representation of the meson (M_2).

the meson-baryonium mixing.

This mixing obviously cannot occur at the lowest topological entropy because of the different colors of the two continuous lines in a baryonium state. It can be realized only via nonplanar connections, e.g., through the twisted baryon loops shown in Fig. 6.

The nonplanar baryonium-baryonium connection involves, in addition to the six twisted baryon loops shown in Fig. 6, two other types of loops shown in Fig. 7. All these eight twisted baryon loops have in common the fact that they preserve the clockwise order of color labels in baryons and the anticlockwise order of color labels in antibaryons and they do not introduce singular topological points on the corresponding quantum surfaces. Examples of loops involving crossing of topological flavor lines which lead to singular topological points (and which are therefore ignored in the present model) are shown in Fig. 8.

The occurrence of singular topological points on the quantum surface is easily visualized in Fig. 8: The points denoted by 1, 2, 3, 4 are all identified to one point. Such an identification of more than two points never occurs in Figs. 6 and 7.

Chains involving a higher number of twisted baryon loops will obviously correspond to a higher topological complexity. They will involve topological flavor loops but never color loops. In spite of the fact that the topological expansion in the case of baryons is not a $1/N_f$ expansion,[6] the number N_f of different flavors will still play an important role in the renormalization of Reggeon propagators via the nonplanar $B\bar{B}$ loop insertions, which will be studied in Sec. III.

III. NONPLANAR $B\bar{B}$ LOOP INSERTIONS IN REGGEON PROPAGATORS

We consider now the effect of all possible $B\bar{B}$ loop insertions in the M_2 $(q\bar{q})$ and M_4 $(qq\bar{q}\bar{q})$ propagators. We consider only Reggeons of nonzero isospin. In the case of M_2 we take the flavor of q different from the flavor of $\bar{q}$ and in the case of M_4 we take only those baryonia which can communicate with the M_2, i.e., the flavors of only one

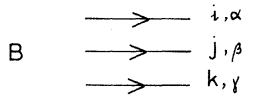

FIG. 4. Quasiplanar representation of the baryon (B).

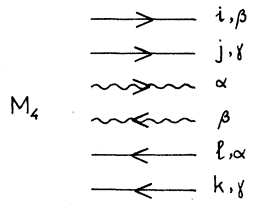

FIG. 5. Quasiplanar representation of the baryonium (M_4).

$q\bar{q}$ pair are identical. The neutral members of the same multiplets will obviously involve the same kind of diagrams.

We note that since none of these $B\bar{B}$ insertions can interchange a quark with an antiquark, all Reggeons of both positive and negative charge conjugation will be shifted in the same direction.

We introduce the following notation (see Fig. 9): the $B\bar{B}$ loop will be denoted by a circle, the $M_2B\bar{B}$ coupling by a dot, the $M_4B\bar{B}$ coupling by two dots, the M_2 planar propagator by a single solid line and the M_4 planar propagator by a double solid line. Sometimes we will use M_2 and M_4 to denote the M_2 and M_4 propagators.

In this notation, the first contribution to the M_2 propagator is shown in Fig. 10. An explanation of the fact that there is no contribution at the one-loop level is given in the Appendix.

Since the nonplanar $B\bar{B}$ loops will mix the M_2 and M_4 states, we consider the Reggeon propagators and the different insertions in these propagators as elements of 2×2 matrices in the space spanned by M_2 and M_4.

The planar propagator is

$$P=\begin{pmatrix} M_2 & 0 \\ 0 & M_4 \end{pmatrix} \tag{1}$$

and we denote by X the matrix which generates all insertions (see Fig. 11). Then, the renormalized (nonplanar) propagator matrix, taking into account all possible insertions, will be

$$P'=P+P\sum_{l=1}^{\infty}(XP)^l . \tag{2}$$

In order to express everything in a compact form, we consider the classes of diagrams denoted by C, $A_{M_2\to M_4}$, $A_{M_4\to M_2}$, and D in Fig. 12. It is clear that C connects M_2 with M_2, D connects M_4 with M_4 and the two A's connect M_2 with M_4. Also, as expected for physical reasons, one can verify explicitly that

$$A_{M_2\to M_4}=A_{M_4\to M_2}\equiv A . \tag{3}$$

Using the notation introduced above we have

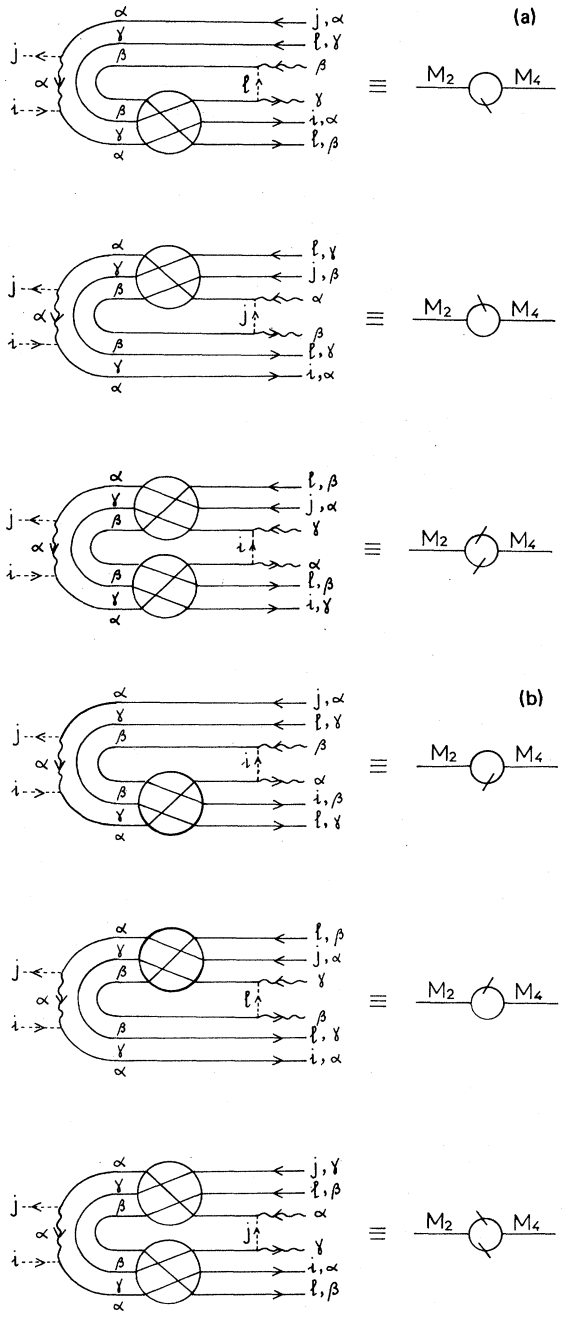

FIG. 6. Twisted $B\bar{B}$ loops connecting M_2 to M_4.

$$P'=\begin{pmatrix} \dfrac{M_2}{1-CM_2} & \dfrac{M_2AM_4}{1-CM_2} \\ \dfrac{M_4AM_2}{1-CM_2} & M_4DM_4+\dfrac{M_4AM_2AM_4}{1-CM_2} \end{pmatrix} . \tag{4}$$

For simplicity we calculate the contributions of the diagrams in a one-dimensional t-independent factorizable model, which has been very success-

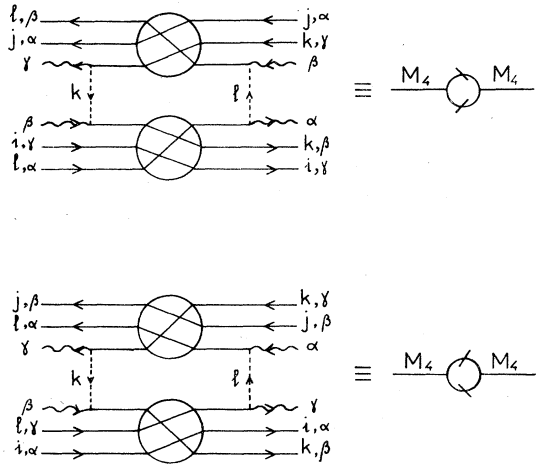

FIG. 7. Two twisted $B\bar{B}$ loops connecting M_4 to M_4.

ful recently in illustrating different aspects of the dual topological unitarization scheme.[13] The values for propagators, couplings, and loops in this model are given in Fig. 9, where α_{M_2}, α_{M_4}, and α_B are the intercepts of the planar M_2, M_4, and B trajectories.

The calculation of C, A, and D in terms of α_{M_2}, α_{M_4}, α_B, g, g', and N is presented in the Appendix. We obtain the following expressions:

$$C=\frac{2g^2}{j-2\alpha_B+1}\frac{1}{\Delta}x(1-x)\left(5-4x+36\frac{x}{N^2}\right), \tag{5}$$

$$A=\frac{gg'}{j-2\alpha_B+1}\frac{N}{[2(N-1)]^{1/2}}\frac{1}{\Delta}(3-2x)\left(1-x+4\frac{x}{N}\right) \tag{6}$$

and

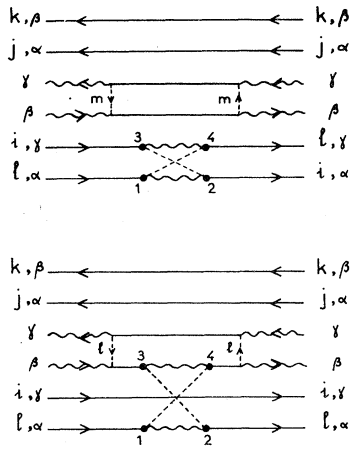

FIG. 8. Examples of twisted $B\bar{B}$ loops forbidden in our model.

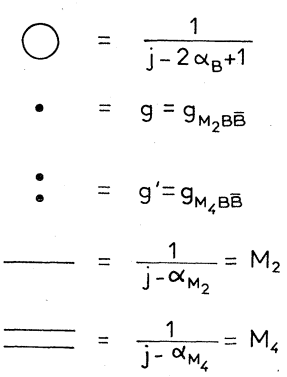

FIG. 9. Notations and explicit expressions for loops, couplings, and propagators.

$$D=(j-\alpha_{M_4})\frac{N}{4(N-1)}\frac{1}{\Delta}\left(1-\frac{2x}{N}\right)^{-1}$$
$$\times\left\{(1-x)(4-x)+\frac{2}{N}[-2+4x+x^2(3-x)]\right.$$
$$\left.-16\frac{x^2}{N^2}\left(1-\frac{1}{N}\right)(3-x)\right\}, \tag{7}$$

where

$$a=\frac{g'^2}{(j-2\alpha_B+1)(j-\alpha_{M_4})}, \tag{8}$$

$$x=aN \tag{9}$$

and

$$\Delta=(1-x)^2-4\frac{x^2}{N^2}(3-x). \tag{10}$$

The compact expressions above are valid provided some convergence conditions are satisfied. These conditions will be discussed and exploited in Sec. IV.

The poles in the new propagator matrix P' are the poles of the determinant of P'. We have

$$\det P'=\frac{M_2M_4{}^2D}{1-CM_2}. \tag{11}$$

We have verified that the poles arise only from the vanishing of the denominator. Thus we find eight poles, which can be obtained by solving the equation

$$j=\alpha_{M_2}+C(j), \tag{12}$$

where $C(j)$ is given by Eqs. (5) and (8)–(10).

By diagonalizing the matrix P' we can get the mixing between M_2 and M_4 (we stress again that

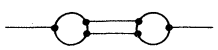

FIG. 10. The first insertion into the M_2 propagator.

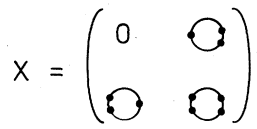

FIG. 11. Graphical representation of the matrix which generates all insertions by iteration.

this mixing is valid only for Reggeons with nonzero isospin). The mixing angle is given by

$$\tan 2\theta = \frac{2M_2 A M_4}{M_4^2 D(1-CM_2) + M_4^2 A^2 M_2 - M_2} . \tag{13}$$

At the renormalized pole position

$$\tan 2\theta = \frac{2AM_4}{M_4^2 A^2 - 1} . \tag{14}$$

We present a discussion of the renormalized poles in Sec. IV. Namely, we discuss the variation of the leading pole position and of the mixing angle as function of g, g', and N and study the restrictions on these variables when we require small shifts and small mixing.

IV. DISCUSSION OF THE RESULTS AND NUMERICAL ESTIMATES

In order to obtain the compact expressions for C, A, and D, certain convergence conditions have to be satisfied. Namely, the convergence of the power series in aR [see Eqs. (A14) and (A15)] is ensured if we require that the modulus of each eigenvalue of the matrix aR be smaller than 1. The eigenvalues are the solutions of the following characteristic equation:

$$\lambda^4 - 2a(N+1)\lambda^3 + a^2(N-2)(N+6)\lambda^2 + 2a^3(12+2N-N^2)\lambda - 8a^4 N = 0 . \tag{15}$$

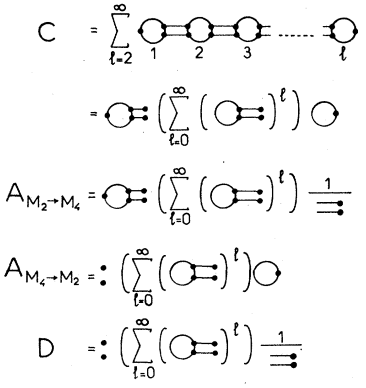

FIG. 12. Graphical representation of C, A, and D (see text).

One solution of this equation is

$$\lambda = 2a \tag{16}$$

which implies

$$a < \tfrac{1}{2} . \tag{17}$$

The other three eigenvalues are the solutions of an equation of third degree:

$$\lambda^3 - 2aN\lambda^2 + a^2(N^2-12)\lambda + 4a^3 N = 0 . \tag{18}$$

This equation has three different real solutions: one negative and two positive solutions.

In terms of the coefficients of Eq. (18) the convergence conditions are expressed as:

$$aN < 1 , \tag{19}$$

$$a^2(N^2-12) < 1 , \tag{20}$$

$$4a^3 N < 1 . \tag{21}$$

Furthermore, from the condition that the left-hand side of Eq. (18) be positive for $\lambda = 1$, we derive the inequality

$$a < \frac{1}{2\sqrt{3}} \tag{22}$$

which is more restrictive than (17). These conditions impose certain restrictions on the values of $g'^2 N$ as we shall show later.

We now study the behavior of the mixing angle [Eq. (13)] in the large-N limit. From the planar bootstrap equation[1] we expect, in this limit, $g'^2 \propto 1/N$. We note that this behavior of g'^2 involves the highest power of N allowed by the convergence condition (19).

It is reasonable to assume also that $g^2 \propto 1/N^2$. For simplicity, we take[14]

$$g'^2 = \frac{K'}{N} , \quad g^2 = \frac{K}{N^2} . \tag{23}$$

Then it is easy to see that $C \propto 1/N^2$, $A \propto 1/N$, and $D \propto$ const. Therefore the mixing angle θ [Eq. (13)] vanishes in the large-N limit. In other words, the physical states become pure $q\bar{q}$ or pure $qq\bar{q}\bar{q}$ states.

We now study the more realistic case $N=3$. This case can be considered as either an SU(3) flavor-symmetric theory or a strongly broken SU(N) where 3 is the "effective" number (N_{eff}) of flavors.

It is interesting to note that the convergence condition (19) implies [with the definitions (8) and (23)] an upper bound for the constant K':

$$K' < (j - \alpha_{M_4})(j - 2\alpha_B + 1) . \tag{24}$$

Taking the planar values α_{M_4} and α_B in the following range:

$$-0.5 \leq \alpha_{M_4} \leq -1 \text{ and } -0.25 \leq \alpha_B \leq 0.15 \tag{25}$$

and imposing the renormalized meson pole to be near $\frac{1}{2}$, one gets

$$K' \lesssim 3 \tag{26}$$

which is obeyed by the value obtained from the planar bootstrap ($K' \simeq 1$).[7] In fact, by studying numerically the convergence region for C [Eq. (5)] one gets $K' \lesssim 1$. Requiring now that C be small ($C \simeq 0.05$) and taking a realistic value[7] for g^2 ($g^2 \simeq \frac{1}{20}$), we further restrict the domain of K' to

$$K' \lesssim 0.3 \tag{27}$$

(this upper bound is in fact even smaller for α_B positive).

These numerical estimates show that if we insist on having K' near 1, we must have $N_{\text{eff}} > 3$. The same conclusion can be reached by a similar numerical study of a renormalized baryonium trajectory near α_{M_4}.

It is interesting to note that for $N=3$, $g^2 \simeq \frac{1}{20}$, $K' \lesssim 0.3$ [Eq. (27)], and α_{M_4} and α_B in the range given by (25), we obtain for the renormalized pole near $\frac{1}{2}$ a mixing angle [see Eq. (14)] smaller than 10°. It is reassuring that we find a connection between small shift and small mixing, a property which is not apparent from our formalism.

V. CONCLUSIONS

In this paper we formulate a DTU model for mesons, baryons, and baryonium which takes into account the new concept of a "quantum" surface and which allows us to investigate in a quantitative and global way the problem of nonplanar insertions in Reggeon propagators. We found a method for calculating in a compact form the effects of summing over all twisted-baryon-antibaryon-loop insertions in the nonzero-isospin Reggeon propagators.

The more complicated problem of the renormalization of the isospin-zero Reggeons has to be solved before drawing detailed phenomenological conclusions. However, we can make some estimates of practical importance.

Namely, we show that our calculation leads to realistic consequences such as restrictions on the value of the baryonium-baryon-antibaryon planar coupling in agreement with the expectation of the planar bootstrap, and restrictions on the effective number of flavors. We also show that small shifts of the planar Reggeon intercepts are naturally expected in the framework of our calculation.

ACKNOWLEDGMENTS

We wish to thank Professor L. A. P. Balázs for many useful discussions. We also thank Professor G. F. Chew, Professor V. Poenaru, and Professor H. P. Stapp for clarifying discussions on the topological aspects of DTU and Professor C. E. Jones for a constructive reading of the manuscript. One of us (J.U.) would like to thank Professor R. Vinh Mau for the kind hospitality at the Institut de Physique Nucléaire, Orsay. This work was supported in part by the National Science Foundation under Grant No. PHY80-07643.

APPENDIX

We present here the explicit calculation of C, D, and A, introduced in Sec. III.

In terms of the twists considered in Sec. II, we identify three classes of $B\bar{B}$ loops, denoted by L_+, L_-, and L_0 in Fig. 13. The spiral line in Fig. 13 represents either an M_2 or an M_4 propagator.

All loops can connect M_4 to M_4 but only the L_+ or L_- loops can connect M_2 to M_4 and only the L_0 loops can connect M_2 to M_2. However, it is easy to see that the L_0 loops can connect M_2 to M_2 only when the flavors of the q and $\bar{q}$ in the M_2 are the same, i.e., only for isospin-zero Reggeons. In the case treated in this paper, $I \neq 0$ Reggeons, there is no $B\bar{B}$-loop insertion in the M_2 propagator at the one-loop level.

For the M_4, in terms of flavor, we distinguish the eight possibilities A_L, A_R, S_E, S_I, A_L^i, A_R^i, S_E^i, and S_I^i shown in Fig. 14. Obviously, $A_{R,L}$ and $S_{E,I}$ contain $N-2$ terms, where N is the total number of flavors. We then introduce a notation which indicates the A or S type and the type of loop which connects the M_4 with M_2. For example, $A_L L_+$ means an M_4 of A_L type which, when followed by a loop of L_+ type, will lead to an M_2.

Our definition of a normalized M_4 state is

$$\begin{aligned} M_4 = \frac{1}{[8(N-1)]^{1/2}} (&A_R L_+ + A_L L_- + A_R L_- + A_L L_+ \\ &+ S_E L_+ + S_I L_- + S_E L_- + S_I L_+ \\ &+ A_R^i L_+ + A_L^i L_- + A_R^i L_- + A_L^i L_+ \\ &+ S_E^i L_+ + S_I^i L_- + S_E^i L_- + S_I^i L_+) . \end{aligned} \tag{A1}$$

The transition between M_2 and M_4 (one loop only, i.e., the beginning of the chain) is given in Table I, the transition between M_4 and M_4, in Table II, and the transition between M_4 and M_2 (end of the chain), in Table III.

We consider now in detail the calculation of C (see Fig. 12):

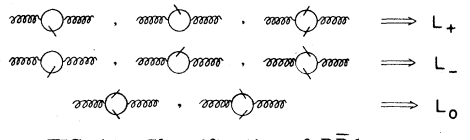

FIG. 13. Classification of $B\bar{B}$ loops.

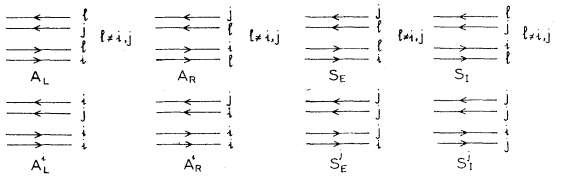

FIG. 14. Definition of the different flavor configurations of M_4.

TABLE I. The number of A's and S's obtained from M_2 followed by a twisted $B\bar{B}$ loop.

Loop	A_R	A_L	S_E	S_I	A_R^i	A_L^i	S_E^j	S_I^j
L_+	1	2	0	0	1	2	2	1
L_-	2	1	0	0	2	1	1	2

$$C = g\frac{g'^2}{(j-2\alpha_B+1)(j-\alpha_{M_4})}\left\{\sum_{l=0}^{\infty}\tilde{n}_l\left[\frac{g'^2}{(j-2\alpha_B+1)(j-\alpha_{M_4})}\right]^l\right\}\frac{1}{j-2\alpha_B+1}g$$
$$= \frac{g^2 a}{j-2\alpha_B+1}\sum_{l=0}^{\infty}\tilde{n}_l a^l, \tag{A2}$$

where a has been defined in Eq. (8) and $\tilde{n}_l$ is the total number of diagrams at the $(l+2)$ loop level. In order to find $\tilde{n}_l$ we look first at the structure of the diagrams constituting C. A careful analysis shows the existence of a very important "triality" property. Namely, by assigning an additive number t to the different loops, such that $t=+1$ for the L_+ loops, $t=-1$ for the L_- loops, and $t=0$ for the L_0 loops, the triality property simply states that in order to have a C chain, the total t value must be zero (mod. 3). We illustrate this property at the two- and three-loop level in Fig. 15.

We would like to underline that this triality property is at the very root of the possibility of obtaining compact forms for our expressions. We recall that this is directly connected to the topological index σ referred to in Sec. II.

Using the triality property and Table II we can

TABLE II. The number of A's and S's obtained from a given type of M_4 followed by a twisted $B\bar{B}$ loop.

	Loop	A_R	A_L	S_E	S_I	A_R^i	A_L^i	S_E^j	S_I^j
A_R	L_+	0	$N-2$	1	1	0	$N-2$	$N-2$	0
	L_-	0	0	1	1	0	0	0	0
	L_0	0	0	0	0	0	0	0	0
A_L	L_+	0	0	1	1	0	0	0	0
	L_-	$N-2$	0	1	1	$N-2$	0	0	$N-2$
	L_0	0	0	0	0	0	0	0	0
S_E	L_+	1	1	0	0	0	0	0	0
	L_-	1	1	0	0	0	0	0	0
	L_0	0	0	0	$N-2$	0	$N-2$	0	$N-2$
S_I	L_+	1	1	0	0	0	0	0	0
	L_-	1	1	0	0	0	0	0	0
	L_0	0	0	$N-2$	0	$N-2$	0	$N-2$	0
A_R^i	L_+	0	1	0	0	1	2	1	0
	L_-	0	0	0	0	1	1	0	0
	L_0	0	0	0	1	0	1	0	1
A_L^i	L_+	0	0	0	0	1	1	0	0
	L_-	1	0	0	0	2	1	0	1
	L_0	0	0	1	0	1	0	1	0
S_E^j	L_+	0	0	0	0	0	0	1	1
	L_-	1	0	0	0	1	0	1	2
	L_0	0	0	0	1	0	1	0	1
S_I^j	L_+	0	1	0	0	0	1	2	1
	L_-	0	0	0	0	0	0	1	1
	L_0	0	0	1	0	1	0	1	0

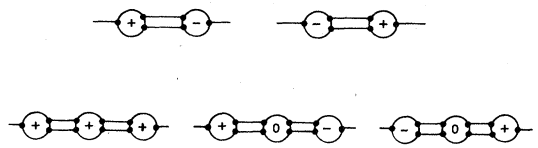

FIG. 15. Illustration of the triality property at the two- and three-loop level.

calculate the number n_{l+1} of M_4's after $l+1$ loops in terms of the number n_l of M_4's after l loops. We find

$$\begin{aligned}
\nu_1^{l+1} &= n_{l+1}(A_R L_+ + A_L L_-) = 2\nu_3^l ,\\
\nu_2^{l+1} &= n_{l+1}(A_R L_- + A_L L_+)\\
&= (N-2)\nu_2^l + 2\nu_3^l + 2\nu_5^l ,\\
\nu_3^{l+1} &= n_{l+1}(S_E L_+ + S_I L_-)\\
&= \nu_1^l + \nu_2^l + (N-2)\nu_3^l + \nu_4^l + \nu_5^l ,\\
\nu_4^{l+1} &= n_{l+1}(A_R^i L_+ + A_L^i L_-)\\
&= (N-2)\nu_3^l + 2\nu_4^l + 2\nu_5^l ,\\
\nu_5^{l+1} &= n_{l+1}(A_R^i L_- + A_L^i L_+)\\
&= (N-2)\nu_2^l + (N-2)\nu_3^l + 2\nu_4^l + 4\nu_5^l ,
\end{aligned} \tag{A3}$$

where we used the relations

$$\begin{aligned}
n_l(S_E L_+ + S_I L_-) &= n_l(S_E L_- + S_I L_+) ,\\
n_l(A_R^i L_+ + A_L^i L_-) &= n_l(S_E^j L_- + S_I^j L_+) ,\\
n_l(A_R^i L_- + A_L^i L_+) &= n_l(S_E^j L_+ + S_I^j L_-) .
\end{aligned} \tag{A4}$$

Since

$$\nu_5^l = -\nu_1^l + \nu_2^l + \nu_4^l \tag{A5}$$

we finally find the following system of equations:

$$\begin{aligned}
\nu_1^{l+1} &= 2\nu_3^l ,\\
\nu_2^{l+1} &= -2\nu_1^l + N\nu_2^l + 2\nu_3^l + 2\nu_4^l ,\\
\nu_3^{l+1} &= 2\nu_2^l + (N-2)\nu_3^l + 2\nu_4^l ,\\
\nu_4^{l+1} &= -2\nu_1^l + 2\nu_2^l + (N-2)\nu_3^l + 4\nu_4^l ,
\end{aligned} \tag{A6}$$

which leads to

$$\begin{pmatrix} \nu_1^{l+1} \\ \nu_2^{l+1} \\ \nu_3^{l+1} \\ \nu_4^{l+1} \end{pmatrix} = \begin{pmatrix} 0 & 0 & 2 & 0 \\ -2 & N & 2 & 2 \\ 0 & 2 & N-2 & 2 \\ -2 & 2 & N-2 & 4 \end{pmatrix}^{l+1} \begin{pmatrix} \nu_1^0 \\ \nu_2^0 \\ \nu_3^0 \\ \nu_4^0 \end{pmatrix} . \tag{A7}$$

When we start with M_2, Table I implies

$$\nu_1^0 = 4 , \quad \nu_2^0 = 2 , \quad \nu_3^0 = 0 , \quad \nu_4^0 = 4 . \tag{A8}$$

When we start with M_4, the definition (A1) gives

$$\nu_1^0 = \nu_2^0 = \nu_3^0 = \nu_4^0 = 2 . \tag{A9}$$

When we end with an M_2, the total number of diagrams is found by summing over all final M_4 and

TABLE III. The number of M_2's obtained from a given type of M_4 followed by a twisted $B\bar{B}$ loop.

	Loop	M_2
A_R	L_+	$2(N-2)$
	L_-	$N-2$
A_L	L_+	$N-2$
	L_-	$2(N-2)$
S_E	L_+	0
	L_-	0
S_I	L_+	0
	L_-	0
A_R^i	L_+	2
	L_-	1
A_L^i	L_+	1
	L_-	2
S_E^j	L_+	1
	L_-	2
S_I^j	L_+	2
	L_-	1

then using Table III:

$$\tilde{n}_l = (2(N-3), N, 0, 6) \begin{pmatrix} \nu_1^l \\ \nu_2^l \\ \nu_3^l \\ \nu_4^l \end{pmatrix} . \tag{A10}$$

Finally, when we end with M_4, we simply sum over the final number of M_4's:

$$\tilde{n}_l = (N-4, N, 2(N-2), 4) \begin{pmatrix} \nu_1^l \\ \nu_2^l \\ \nu_3^l \\ \nu_4^l \end{pmatrix} . \tag{A11}$$

Coming back to the calculation of C we need $\sum_{l=0}^{\infty} \tilde{n}_l a^l$, $\tilde{n}_l$ being written as

$$\tilde{n}_l = (2(N-3), N, 0, 6) R^l \begin{pmatrix} 4 \\ 2 \\ 0 \\ 4 \end{pmatrix} , \tag{A12}$$

where

$$R = \begin{pmatrix} 0 & 0 & 2 & 0 \\ -2 & N & 2 & 2 \\ 0 & 2 & N-2 & 2 \\ -2 & 2 & N-2 & 4 \end{pmatrix} . \tag{A13}$$

Then

$$\sum_{l=0}^{\infty} \tilde{n}_l a^l = (2(N-3), N, 0, 6) \sum_{l=0}^{\infty} (aR)^l \begin{pmatrix} 4 \\ 2 \\ 0 \\ 4 \end{pmatrix} \tag{A14}$$

$$= (2(N-3), N, 0, 6) \frac{1}{1-aR} \begin{pmatrix} 4 \\ 2 \\ 0 \\ 4 \end{pmatrix} . \tag{A15}$$

We note that the relation (A14) can be written as (A15) if some convergence conditions are satisfied. These conditions were discussed in Sec. IV.

Performing the remaining algebra we obtain the expression for C given in formula (5) in Sec. III.

Similarly we obtain the expressions (6) and (7) for A and D, respectively.

*On leave of absence from Physics Department, University of Nebraska, Lincoln, NE 68588.
†Laboratoire associé au CNRS.
‡Postal address: Tour 16-El, 4 Place Jussieu 75230 Paris Cedex 05, France.

[1]G. F. Chew and C. Rosenzweig, Phys. Rep. 41, 263 (1978).
[2]G. C. Rossi and G. Veneziano, Nucl. Phys. B123, 507 (1976); L. Montanet, G. C. Rossi, and G. Veneziano, Phys. Rep. 63, 149 (1980); M. Imachi, S. Otsuki, and F. Toyoda, Prog. Theor. Phys. 55, 551 (1976); 55, 1211 (1976); 57, 517 (1977); F. Toyoda and M. Uehara, *ibid.* 58, 1456 (1977); M. Uehara, *ibid.* 59, 1587 (1978).
[3]K. Konishi, Nucl. Phys. B131, 143 (1977); H. P. Stapp, Lett. Nuovo Cimento 19, 622 (1977); F. Capra, Phys. Lett. 68B, 93 (1977).
[4]G. F. Chew, Nucl. Phys. B151, 237 (1979); Phys. Lett. 82B, 439 (1979); see also G. F. Chew, J. Finkelstein, J. P. Sursock, and G. Weissmann, Nucl. Phys. B136, 493 (1978).
[5]G. F. Chew, B. Nicolescu, J. Uschersohn, and R. Vinh Mau, CERN Report No. TH-2635, 1979 (unpublished); B. Nicolescu and J. Uschersohn, in *Quarks, Gluons, and Jets*, proceedings of the XIV Rencontre de Moriond, Les Arcs, Savoie, France, 1979, edited by J. Trân Thanh Vân (Editions Frontieres, Dreux, France, 1979), p. 63.
[6]G. F. Chew and V. Poenaru, Phys. Rev. Lett. 45, 229 (1980); Lawrence Berkeley Laboratory Report No. LBL-11433, 1980 (unpublished).
[7]H. M. Chan and S. T. Tsou, Nucl. Phys. B118, 413 (1977).
[8]B. R. Webber, Phys. Lett. 62B, 449 (1976); J. G. Rushbrooke and B. R. Webber, Phys. Rep. 44, 1 (1978).
[9]T. H. Hannson, Rutherford Laboratory Report No. RL-78-105, 1978 (unpublished); N. A. Papadopoulos, Nucl. Phys. B134, 105 (1978); M. Uehara, Saga University Report No. SAGA-HE-7, 1980 (unpublished).
[10]R. V. Gavai and D. P. Roy, Nucl. Phys. B137, 301 (1978); Phys. Lett. 82B, 139 (1979); R. V. Gavai, Nucl. Phys. B162, 350 (1980); Phys. Rev. D (to be published).
[11]L. A. P. Balázs and B. Nicolescu, Z. Phys. C 6, 269 (1980).
[12]In other words, we consider here only the nonzero-isospin Reggeons. For zero-isospin Reggeons an analogous hypothesis can be made, namely, the conservation of the minimal number (two) of singular points.
[13]N. Sakai, Nucl. Phys. B99, 167 (1975); M. Fukugita, T. Inami, N. Sakai, and S. Yazaki, *ibid.* B121, 93 (1977); J. Uschersohn, *ibid.* B114, 137 (1976); S. Jadach, *ibid.* B99, 514 (1975).
[14]C. E. Jones and J. Uschersohn, Phys. Lett. 89B, 409 (1980).